International Journal of Applied Engineering Research ISSN 0973-4562 Volume 10, Number 22 (2015) pp 43239-43243

Modeling Of Heat And Mass Transportation In The Keyhole Of 316l Stainless Steel And Steel Joints During Pulsed Nd: Yag Laser Welding

K. Suresh Kumar

University of Madras, Chennai Tamil Nadu, India-600005 Email: lectsuresh25@gmail. com

A. Jayanthi

Jeppiaar Institute of Technology, Chennai Tamil Nadu, India-631604 Email: jayanthi@jeppiaarinstitute. org

Abstract
A finite element based three-dimensional model was developed to investigate the heat and mass transfer across weldpool of similar and dissimilar combinations of 2 mm thick 316 L stainless steel and mild steel joints made using pulsed Nd: YAG laser welding. The convective and conductive heat transfer in vapour-liquid boundary and liquid-solid boundary were investigated using the keyhole models simulated in terms of Peclet number for all weld joints considered. The simulated results are compared and discussed with experimental observations found that have close association with each other.

Keywords: laser welding, stainless steel, mild steel, temperature distribution, Peclet number, keyhole

1. Introduction

Laser welding has been received much attention as a promising joining technology because of its less heat input and low distortion. In industries, dissimilar welding of stainless steel and steel alloys find variety of applications due to the need to tailor the location of materials where a transition in mechanical properties, temperature, pressure, and/or performance in service is required. Dissimilar welding have been processed through explosion welding, pressure welding, friction welding, and soldering and brazing, but very few dissimilar welding done using laser as heat source. For example, 304L stainless steel-12L13 stainless steel [1], INCONEL 600-INCONEL 690 [2], hard metals (K40, K10)-Steel (DIN 17007) [3], steel-kovar, copper-steel and copper–Aluminium [4] and 316LN-IG steel [5]. Very limited work has been attempted to made dissimilar welding of AISI 316L stainless steel and steel using pulsed Nd: YAG laser welding. Owing to the wide range of uses of dissimilar joints and numerous advantages of laser welding, it is essential to understand the heat and mass transfer involved in the keyhole that enable deep penetration and efficient welding of thick sections using pulsed Nd: YAG laser welding.

The literatures those dealt with fundamental science of heat and mass transfer by numerical and analytical models are compiled in the years 1986 [6], 1995 [7] and 2004 [8]. The thermal modeling of laser welding and its related processes such as alloying, cladding and surface hardening were reviewed up to the year 2002 [9]. It has found that those models have developed and simulated to investigate the thermal profile, melt flow and heat transfer in the weldpool. For instance, temperature distribution, residual stress and distortion distributions are evaluated for austenitic stainless steel [10], a 2D model was developed to investigate the laser-material interaction of a pulsed laser [11], a 3D analytical model for laser material-interaction for spatial and temporal distributed heat source [12], two sets of 3D models was developed for turbulence on the transportation characteristics associated with typical laser welding process [13] and a control volume method approach was introduced to discretize the governing equation for laser heating of semi-infinite solid with consecutive pulses [14]. The most recent heat transfer models using numerical/analytical methods on laser beam welding process were briefed up to date [11] and [15]. However, it has found that very few reports about the heat and melt flow during pulsed laser welding on AISI 316L stainless steel-steel joints.

Many simulation codes have been developed for laser welding based on finite difference, finite element, or control volume methods. But, newly developed multiphysics software's like LUMET (for laser ultrasonic metallurgy), open FOAM and COSMOL are allow us to simulate the laser welding and its process dynamics [16]. Hence, we had chosen comsol multiphysics code to compute the heat and mass transfer during pulsed Nd: YAG laser welding.

This article presents an investigation on the FEA based heat and mass transfer model developed using comsol multiphysics for similar and dissimilar combinations of 2 mm thick 316 L stainless steel and mild steel joints made using pulsed Nd: YAG laser welding. The simulated convective and conductive heat transfer across the weld pool is compared with metallographic examinations of those keyholes obtained for those combinations from experiments.

2. Experimental methods

AISI 316L stainless steel and mild steel plates having dimensions of 150 mm (Length) x 50 mm (Width) x 2 mm (Thick) with smooth faces that are feasible for butt-welding and its chemical compositions are given in table 1. The Nd: YAG laser beam delivered to the CNC workstation through a fiber optic beam delivery system. The laser beam focused at the focal distance of 200 mm that having the focused waist diameter of 0. 451 mm and targeted vertically on the surface. The laser pulses are assumes as Hermit–Gaussian pulse spatially distributed in TEM00 mode. The Nd: YAG laser

beam attached with highly précised CNC machine for accurate alignment at welding velocity fixed as 180 mm/minutes. High purity of Argon (Ar) used as shielding gas and supplied at the rate of 20 l/min at the top and bottom surface of the plates at an angle 45º and the nozzle placed behind the laser beam. The parameters like peak power, pulse duration and pulse repetition rate are varied until the optimal welding condition to obtain the full penetration without any defects. The optimized parameters are presented as shown in table 2. The similar 316L stainless steel weld electrolytic etched in 10% oxalic acid, mild steel weld electrolytic etched in Nital to expose the features of weldpool in weld joints.

Table 1: Chemical compositions of sample materials

Elements	C	Si	Mn	P	S	Ni	Cr	Mo	Balance
316L SS	0. 022	0. 411	0. 615	0. 040	0. 016	10. 68	16. 85	2. 112	Fe
MS	0. 07	0. 04	0. 20	0. 008	0. 009	-	-	-	Fe

Table 2: Parameters used for pulsed Nd: YAG laser welding

Parameters	Values	Units
Average Peak Power for Similar 316L stainless steel, Similar mild steel, Dissimilar 316L stainless steel-mild steel and Dissimilar 316L stainless steel-mild steel (with offset-ted beam position)	2100, 2050, 2200 and 2200	Watts
Pulse energy	25. 2, 25. 8, 26. 4, 26. 4	Joule's
Heat input	120, 126, 132, 132	J/mm
Pulse duration	12	ms
Frequency	15	Hz
Welding Velocity	3	mm/s
Interaction Time	48	ms
Duty Cycle	18	%
Pulse over lapping	78. 60	%

3. Heat transfer model

In this simulation work, temperature distributions in weld specimen while it exposed to a moving laser beam during welding with known parameters as shown in table 2. The speed of heat conduction depends on the material density, specific heat capacity and thermal conductivity, the difference in temperatures, and the shape of the conductor in principle. Hence, the time dependent heat conduction equation given by

$$\rho c_p \frac{\partial T}{\partial t} + \rho C_p U \nabla T = \nabla(K \nabla T) \text{---} \quad (1)$$

The specimens are happened to be original heat sources during pulsed laser welding process by the phenomenon of laser materials interaction. Therefore, the governing equation for time dependent heat conduction during the pulsed laser welding process given by

$$\rho c_p \frac{\partial T}{\partial t} + \rho C_p U \nabla T = \nabla(K \nabla T) + Q \text{---} \quad (2)$$

The heat input within the specimen by Gaussian distribution is given by

$$Q(x,y,z) = Q_0(1 - R_c).\frac{A_c}{\pi \sigma_x \sigma_y} e - \left[\frac{(x-x_0)}{2\sigma_x^2} + \frac{(y-y_0)}{2\sigma_y^2}\right].e^{-A_c z} \text{---} \quad (3)$$

The heat flux equation for the boundaries given by

$$q_0 = h\,(T_{ext} - T_0) \text{---} \quad (4)$$

Boundary condition for thermal insulation given by

$$-n.(-K \nabla T) = 0 \text{---} \quad (5)$$

In building this model, assumptions made as follows:

- ✓ The problem is a time dependent three-dimensional transient model
- ➢ The heat is lost through radiation to the ambience
- ➢ Nature of the laser beam is pulsed and triangular in shape
- ➢ The electromagnetics of the laser beam is not simulated
- ➢ Laser defocused on the vertically surface
- ➢ Thermophysical properties are depended on temperature
- ➢ Energy distributed spatially in Hermit-Gaussian with TEM_{00} mode
- ➢ No constrains is applied on the edges
- ➢ The ambient temperature assumed as 293 K
- ➢ Autogenous weld (No filler material used)

Based on the numerical results of keyhole models, the convective and conductive heat transfers in various actual keyholes were investigated for different weld joints as discussed.

4. Results and Discussions

In welding, convection is dominant mechanism of heat and mass transfer, many dimensionless numbers that are helps to determine the heat and mass transfer. Paclet number may use to estimate the convective heat transfer relative to the conductive heat transfer at a solid-liquid boundary in a system like keyhole. In these circumstances, heat and mass distributions across the weldpool were predicted in terms of Paclet number distribution that helps to distinguish the solid–liquid boundary of a weldpool and heat affected zone for similar and dissimilar combinations of 2 mm thick 316 L stainless steel and mild steel joints made using pulsed Nd: YAG laser welding. This results and discussions intended on distribution of Peclet number weldpool to investigate heat and mass transportation in all four different joints given as follows.

4. 1 Investigation on the keyhole of similar 316 L stainless steel joint

The various components such as melt flow region, pulse trials, keyhole top, keyhole front, retained vapour region, downward vapour region of a typical keyhole predicted in terms of distribution Peclet number for 316L stainless steel joint as shown in fig. 1. The compressed contour lines reveal the

higher temperature gradient in keyhole front than behind it. But, Paclet number almost remains constant i. e., Pe << 1 throughout the keyhole and no/very less fluctuation observed in the expected keyhole region known assumed as vortex region as shown fig. 2. Here, density of the fluid (melt/vapour) may assumed as constant that lie on a keyhole vortex region at some instant and continued to be lie on the moving vortex line in the welding direction. Thus, vortices and viscous forces confined in to a thin boundary layer on the aerofoil. However, temperature gradients concentration gradient is very high and become time-dependent, hence, net value of heat transportation took place only by the convection where thermal conduction and diffusion is negligible. The strong velocity of up draught of melt flow produces potential rotary motion driven by the buoyancy forces due to the large variation in the temperature and concentration gradients as that of natural convection.

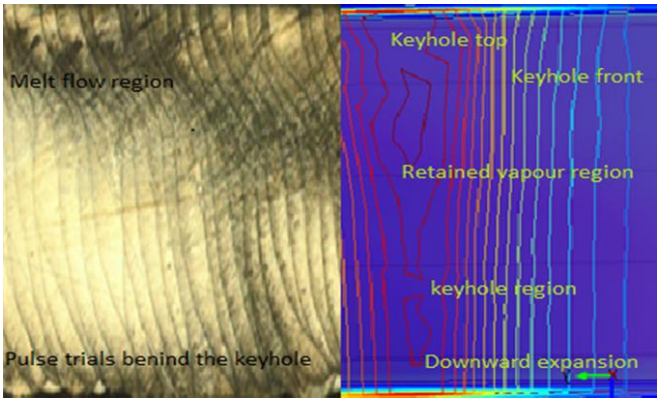

Fig. 1: Simulated contours of Paclet number levied on the actual keyhole (LCS view) of 316 L stainless steel

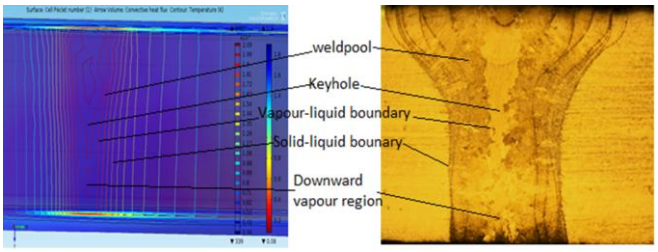

Fig. 2: Contours of Peclet number in 316L stainless steel during pulsed laser welding

However, Islands of contours were observed in the keyhole bottom due to the large velocity fluctuations and there is significant cross-stream motion of fluids in the form of correlated parcels of fluids called eddies. Cross-stream transport in turbulent flow takes place primarily by turbulent vortices, and so the transport rates are much higher than in laminar flow. This turbulence identified in the form of laser-induced vapor generated waves (Gauffers) exerted heat flux towards the depth as that of an actual keyhole as shown in fig. 2. However, this turbulence decreased towards the molten metal, because the vapour cannot penetrate the liquid at the vapour-liquid boundary layers. Therefore, heat and mass transport very close to keyhole boundary takes place by the combination of eddy diffusion and molecular diffusion that shows some discontinuities in the rear and front side of the keyhole region.

In high Peclet number, heat transfer by convection becomes less dominate and dependent of the thermal diffusivities. Hence, heat transfer cannot take place only by the convection, so, there is no fluid flow across the liquid (Melt pool)-solid (HAZ) boundary. However, the convection takes place only in the direction opposite to welding. The temperature and concentration gradients are relatively lesser in radial directions where Peclet number (Pe) >> 1 as shown in fig. 1 and 2. Thermal diffusion takes place in HAZ by laminar flow due to molecular diffusion on front and rear side of the keyhole boundary. Therefore, the rate of heat conduction depends only by the molecular diffusion. This result reveals that the keyhole widened at top, trapped vapor region at the centre and downward expanded vapor region at the bottom of a 316 L stainless steel joint as shown fig. 2.

4. 2 Investigation on the keyhole of similar mild steel joint

Unlike in 316L stainless steel joint, a necking found in the middle of the keyhole region computed for mild steel joint as shown in fig. 3. As a result, larger bent occurs in the keyhole front due to the higher thermal conductivity of the mild steel than the 316L stainless steel. In addition, some fluctuations were found around the necking region on the rear side of the keyhole. The very low Peclet number i. e., Pe<< 1 was observed throughout the keyhole and weldpool region due to the higher thermal conductivity of the mild steel that causes larger weldpool and wider heat affected zone. Therefore, the rate of heat and mass transfer is very high due to the convective heat flow in the keyhole region. Similarly, higher rate of convection and diffusivity in the weldpool and heat flow velocity and diffusivity in heat affected zone as discussed in chapter 4. 1.

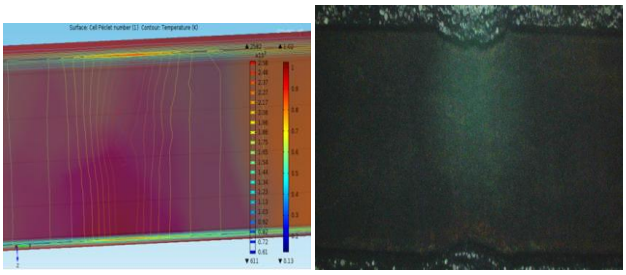

Fig. 3: Contours of Peclet number in mild steel during pulsed laser welding

4. 3 Investigation on the keyhole of 316 L stainless steel-mild steel joint

The distribution of Peclet number computed in terms of convective heat flux for 316L stainless steel-mild steel joint where the laser pulses spotted symmetrically across the butt joint during welding as shown in Fig. 4. The keyhole appeared in usual shape as that of 316L stainless steel, but broadened throughout the thickness compare to both the 316L stainless steel and mild steel joint. The discontinuity in heat flux contours appeared in the keyhole region where the Pe<< 1 due

to the exchange of heat from molten 316L stainless steel to mild steel during welding. Even though, molten 316L stainless steel exchanges heat flux to melt mild steel that results in an incomplete penetration. Since, the mild steel has higher thermal conductivity than the 316L stainless steel, large amount of heat spent for conduction rather melting as shown in fig. 5, hence, an expansion notified in the middle of the keyhole. Thus, achieving full penetration of this dissimilar joint gets affected. The lesser fluctuations appeared in 316L stainless steel than mild steel due to their difference in thermal conductivity.

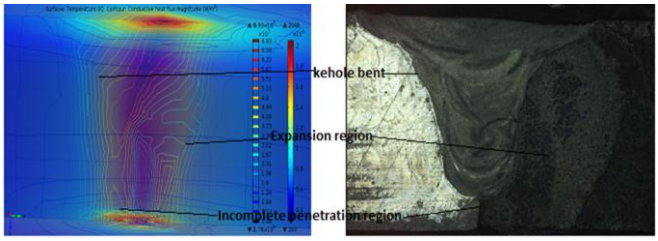

Fig. 4: Contours of Paclet number in 316L stainless steel-mild steel during pulsed laser welding.

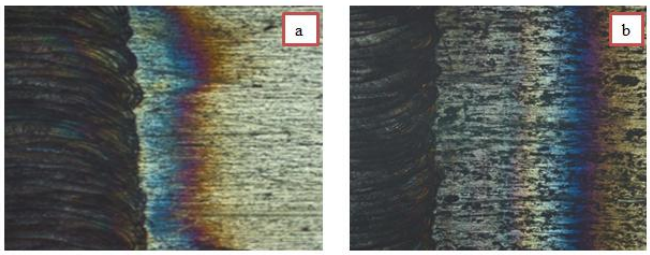

Fig. 5: Temperature Distribution in 316L stainless steel-mild steel with symmetrically focused spot position across butt joint (a) 316L stainless steel side (b) mild steel side.

4. 4 Investigation on the keyhole of 316 L stainless steel-mild steel joint weld with offset-ted beam position

Fig. 6 shows the distribution of Peclet number computed in terms of convective heat flux for 316L stainless steel-mild steel joint where the laser focal position offset-ted towards 316L stainless steel side by 2 µm before welding. Since, more heat input given to the 316L stainless steel than mild steel, large amount of melting occurs and the keyhole appeared as that of similar 316L stainless steel weld. The lesser fluctuation and no signs of necking notified throughout keyhole boundaries. The contours appeared in the keyhole region show some turbulence where the convection is only source of heat transfer in the depth direction. However, no turbulence but the streamline flow of heat transfer observed at the keyhole-melt pool boundary and melt pool-heat affected zone boundary. The molten 316L stainless steel has driven to melt mild steel, therefore, some fluctuation appeared throughout the keyhole boundary due to the higher thermal concentration gradient of molten 316L stainless steel that enable adequate melting in mild steel and achieve keyhole welding. Hence, penetration depth did not affected in this dissimilar weld while welding with offset-ted beam position. Thus, almost equal temperature distribution achieved on each sides of the dissimilar joint with acceptable weld bead as shown in fig. 7.

These observations on temperature distribution predicted by the numerical modeling have close association with experimental results of similar and dissimilar combinations of 2 mm thick 316 L stainless steel and mild steel joints made using pulsed Nd: YAG laser welding.

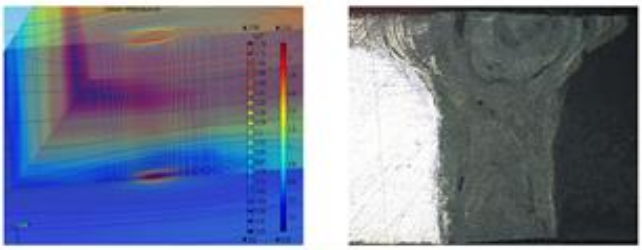

Fig. 6: Contours of Paclet number in 316L stainless steel-mild steel with offset-ted beam position during pulsed laser welding.

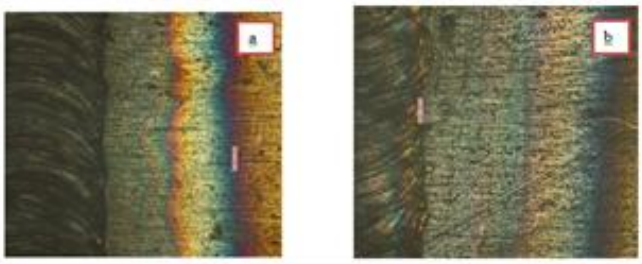

Fig. 7: Temperature Distribution of 316L stainless steel-mild steel with offset-ted laser spot by 2µm towards 316L stainless steel (a) 316L stainless steel side (b) mild steel side.

Conclusion

1. Similar and dissimilar combinations of 2 mm thick 316 L stainless steel and mild steel joints were made using pulsed Nd: YAG laser welding by optimized parameters like average peak power, pulse duration, pulse repetition rate and laser spot position.
2. The heat and mass transfer in keyhole/weldpool of the joints considered for investigations were simulated in terms of Peclet number using finite element based comsol multiphysics code.
3. These simulated and experimental results were compared and investigated on heat and mass transfer drawn the following conclusions on keyhole,

a. . In 316 L stainless steel joint, the keyhole widened at top, trapped vapor region at the centre and downward expanded vapor region at the bottom.

b. In mild steel joint, a strong necking found in the middle of the keyhole, hence larger bent occurs in the keyhole front due to the higher thermal conductivity of the mild steel.

c. In 316L stainless steel-mild steel joint, the keyhole appears wider and an expansion found in the middle due to higher thermal conductivity of mild steel.

Hence, achieving full penetration of this dissimilar joint is affected.

d. In 316L stainless steel-mild steel joint made with offset-ted beam position, large amount of melting occurs in 316L stainless steel than mild steel; hence, the keyhole appeared as that of similar 316L stainless steel weld. The molten 316L stainless steel exchanges heat to mild steel that enable adequate melting and achieve keyhole welding. Hence, penetration depth did not affect.

4. The simulated keyhole models were compared with experimental observations found that those models have close association with experimental weld joints.

Acknowledgement
The author wish to thank Dr. S. Venugopal, Director/MMG, Indira Gandhi Centre for Atomic Research, Kalpakkam, Tamil Nadu, India for granting permission and providing facilities to carry out the experimental work and having fruitful discussions throughout this work.

References

[1] Zhang Li and G. Fontana. Autogenous laser welding of stainless steel to free cutting steel for the manufacturing of hydraulic valves. Journal of materials processing technology, Vol. 74, pp. 174-182, 1998.

[2] W. J. Han, J. G. Byeon and K. S. Park. Welding characteristic of the Inconel plate using a pulsed Nd: YAG laser beam. Journal of materials processing Technology, Vol. 113, pp. 234-237, 2001.

[3] Alexandra P. Costa, Luisa Quintino and Martin Greitmann. Laser beam welding hard metals to steel. Journal of material processing technology, Vol. 141, pp. 163-173, 2003.

[4] A. C. Spowage, T. A. Mai and. Characterization of dissimilar joints in laser welding of steel-Kovar, Copper –Steel and Copper – Aluminium. Material science and engineering A, Vol. 374, pp. 224-233, 2004.

[5] Hirkazu Yamada, Hiroshi Kawamura, Yoshiharu Nagao, Fumiki Takada and Wataru Kohno. Mechanical properties of weldments using irradiated stainless steel welded by the laser method for ITER blanket replacement. Journal of Nuclear Materials, Vol. 355, pp. 119-123, 2006.

[6] E. R. G. Eckert, R. J. Goldstein, E. Pfender, J. W. Ramsey, W. E. Ibele, S. V. Pataankar, T. W. Simson, T. H. Kuehn, P. J. Strykowski, A. Decker, H. O. Lee and S. L. Girshick. Heat transfer – A review of 1986 literature. International journal of heat and mass transfer, Vol. 30 (12), pp. 2449-2523, 1987.

[7] E. R. G. Eckert, R. J. Goldstein, W. E. Ibele, S. V. Pataankar, T. W. Simson, T. H. Kuehn, P. J. Strykowski, K. K. Tamma, J. V. R. Heberlein, J. H. Davidson, J. Bischof, F. A. Kulacki, U. Kortshagen and A. Bar-Cohen. Heat transfer – A review of 2004 literature. International journal of heat and mass transfer, Vol. 42, pp. 2717-2797, 1999.

[8] R. J. Goldstein, W. E. Ibele, S. V. Pataankar, T. W. Simson, T. H. Kuehn, P. J. Strykowski, K. K. Tamma, J. V. R. Heberlein, J. H. Davidson, J. Bischof, F. A. Kulacki, U. Kortshagen, S. Garrick, V. Srinivasan, K. Ghosh and R. Mittal. Heat transfer – A review of 2009 literature International journal of heat and mass transfer, Vol. 53, pp. 4343-4396, 2010.

[9] R. C. Crafer and A. P. Mackwood. Thermal modeling of laser welding and related process: a literature review. Optics & Laser technology, Vol. 37, pp. 99-115, 2005.

[10] K. R. Balasubramanian, G. Buvanashekaran and K. Sankaranarayanasamy. Modeling of laser beam welding of stainless steel sheet butt joint using neural networks. CIRP Journal of manufacturing science and technology, Accepted Manuscript, 2010.

[11] Kamel Abderrazak, Wassim Kriaa, Wacef Ben Salem, Hatem Mhiri, Georges Lepalac and Michel Autric. Numerical and experimental studies of molten pool formation during an interaction of a pulse laser (Nd: YAG) with a magnesium alloy. Optics and laser technology, Vol. 41, pp. 470-480, 2009.

[12] Mihai Oane, Florea Scarlat and Ion N. Mihaliescu. The semi analytical solution of the Fourier heat equation in beam 3D inhomogeneous media interaction. Infrared Physics and technology, Vol. 51, pp. 344-347, 2008.

[13] Chakraborty, Nilanjan Chakraborty and Suman. Modeling of turbulent molten pool convention in laser welding of a copper nickel dissimilar couple. International journal of heat and mass transfer, Vol. 50, pp. 1805-1822, 2007.

[14] S. Z. Shuja, B. S. Yilbas and Shafique M. A. Khan. Laser heating of semi-infinite solid with consecutive pulses: influence of material properties on temperature field. Optics and laser technology, Vol. 40, pp. 472-480, 2008.

[15] Analytical modeling of temperature distribution, peak temperature, cooling rate, and thermal cycles in a solid work piece welded by laser welding process. K. Suresh Kumar, 2014, Procedia Materials Science, Vol. 6, pp. 821 – 834.

[16] D. Ferguson, W. Chen, T. Bonesteel and J. Vosburgh. A look at physical simulation of metallurgical process, past, present and future. Materials science and engineering A, Vol. 499, pp. 329-332, 2009.